Journal of Applied Polymer Science

Effects of Amino-Functionalized Carbon Nanotubes on the Properties of Amine-Terminated Butadiene-Acrylonitrile Rubber-Toughened Epoxy Resins

Jusheng Zhang,[1] Yuting Wang,[1] Xiaoshan Wang,[1] Guowei Ding,[1] Youqiang Pan,[2] Hongfeng Xie,[1] Qingmin Chen,[1] Rongshi Cheng[1,3]

[1]Key Laboratory of High-Performance Polymer Materials and Technology, Ministry of Education, School of Chemistry and Chemical Engineering, Nanjing University, Nanjing 210093, China

[2]National Engineering Laboratory for Advance Road Materials, Jiangsu Transportation Institute, Nanjing 211112, China

[3]College of Material Science and Engineering, South China University of Technology, Guangzhou 510640, China

Correspondence to: H. Xie (E-mail: hfxie@nju.edu.cn)

ABSTRACT: Amino-functionalized multiwalled carbon nanotubes (MWCNT-NH_2s) as nanofillers were incorporated into diglycidyl ether of bisphenol A (DGEBA) toughened with amine-terminated butadiene–acrylonitrile (ATBN). The curing kinetics, glass-transition temperature (T_g), thermal stability, mechanical properties, and morphology of DGEBA/ATBN/MWCNT-NH_2 nanocomposites were investigated by differential scanning calorimetry (DSC), thermogravimetric analysis, a universal test machine, and scanning electron microscopy. DSC dynamic kinetic studies showed that the addition of MWCNT-NH_2s accelerated the curing reaction of the ATBN-toughened epoxy resin. DSC results revealed that the T_g of the rubber-toughened epoxy nanocomposites decreased nearly 10°C with 2 wt % MWCNT-NH_2s. The thermogravimetric results show that the addition of MWCNT-NH_2s enhanced the thermal stability of the ATBN-toughened epoxy resin. The tensile strength, flexural strength, and flexural modulus of the DGEBA/ATBN/MWCNT-NH_2 nanocomposites increased increasing MWCNT-NH_2 contents, whereas the addition of the MWCNT-NH_2s slightly decreased the elongation at break of the rubber-toughened epoxy. © 2014 Wiley Periodicals, Inc. J. Appl. Polym. Sci. **2014**, *131*, 40472.

KEYWORDS: glass transition; graphene and fullerenes; mechanical properties; nanotubes; rubber; thermosets

Received 7 October 2013; accepted 16 January 2014

DOI: 10.1002/app.40472

INTRODUCTION

Because of their good engineering performance, such as their high stiffness and strength, high-temperature performance, creep resistance, chemical resistance, and adhesive properties, epoxy resins are intensively used in many fields, including the surface coatings, structural adhesives, insulating materials, and matrices for fibrous composites. However, the inherent brittleness in the cured solid state due to the high crosslinking density becomes one undesirable property in advanced application use in industry. As such, epoxy resins tend to have poor resistance to crack initiation and growth, and this results in poor impact and peel properties. Therefore, great efforts to improve the toughness of epoxy resins have been made in recent decades.[1] A couple of methods have been proposed to increase the toughness of epoxy resins, including reactive liquid rubber, thermoplastics, interpenetrating polymer networks, thermotropic liquid crystal, and nanofillers.[2–6] Rubber toughening is the most frequently used and widely accepted among these methods. Reactive rubber-toughened epoxy generally has two distinct phases. The larger phase is the base resin, and the minor phase consists of small (on the order of 1 μm in diameter) distributed elastomeric entities. The addition of the second phase significantly improves the fracture toughness by providing crack pinning and stress distribution mechanisms within the material.[7–10] Inevitably, however, the addition of liquid reactive rubber will sacrifice the mechanical properties of the epoxy resin.

Carbon nanotubes (CNTs) and carbon nanofibers are considered as reinforcements for the polymer matrix because of their remarkable physical, chemical, and electrical properties with small dimensions and high aspects.[11–14] To transfer these outstanding properties to modified epoxies, the functionalization of pristine CNTs is essential for getting strong interfacial bonding and proper dispersion.[15–19] Amino functionalization has been developed in recent years to improve the dispersion and interfacial adhesion of CNTs with epoxy resins.[20–27]

The main aim of this study was to further improve the properties of reactive rubber-toughened epoxies through the

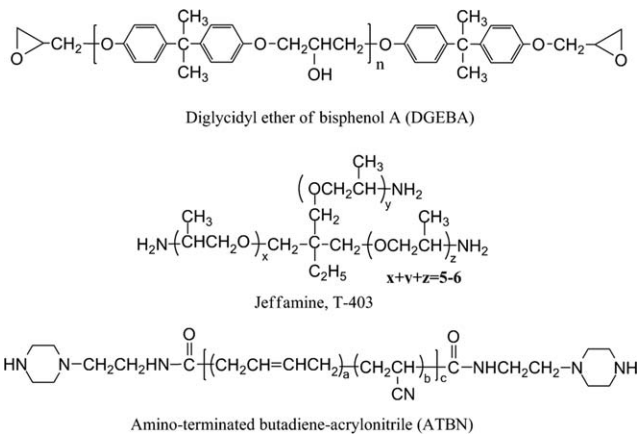

Figure 1. Chemical structures of DGEBA, Jeffamine T-403, and ATBN.

introduction of amino-functionalized CNTs. In this study, a reactive butadiene–acrylonitrile rubber, amine-terminated butadiene–acrylonitrile (ATBN), was chosen as a toughener for epoxy resin. Amino-functionalized multiwalled carbon nanotubes (MWCNT-NH_2s) were incorporated into the toughened epoxy as nanofillers. The curing behaviors, glass-transition temperatures (T_g's), thermal stability, and mechanical properties of the nanocomposites were characterized.

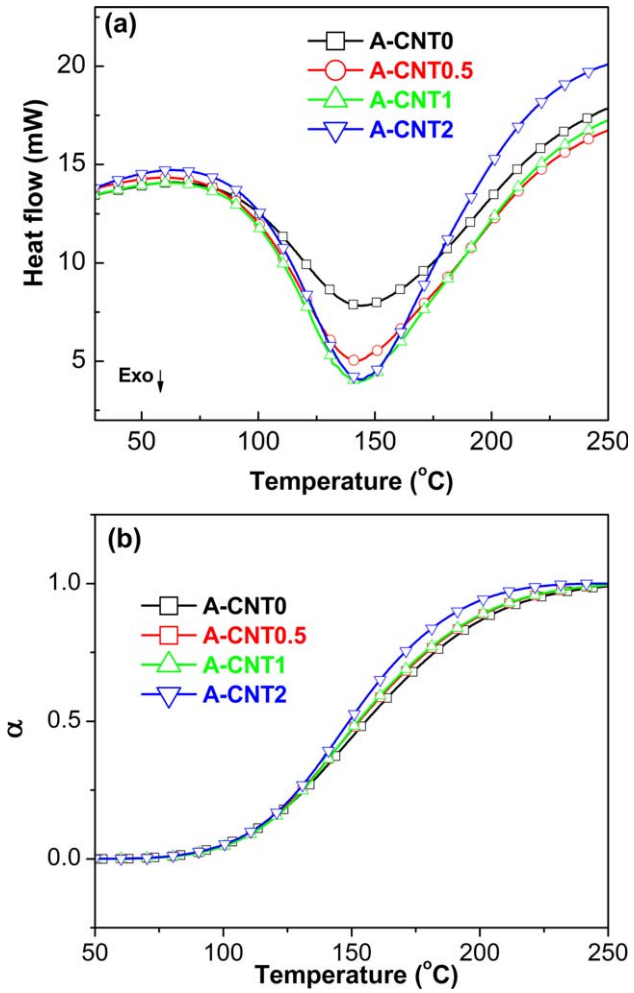

Figure 2. (a) DSC curves and (b) relationship between the conversion (α) and the temperature for the DGEBA/ATBN/MWCNT-NH_2 nanocomposites at a β of 20°C/min. [Color figure can be viewed in the online issue, which is available at wileyonlinelibrary.com.]

Table I. T_i, T_p, and ΔH Values for the DGEBA/ATBN/MWCNT-NH_2 Nanocomposites

MWCNT-NH_2 (wt %)	β (°C/min)	T_i (°C)	T_p (°C)	ΔH (J/g)
0	5	47.7	112.5	212.5
	10	47.6	128.3	239.5
	15	48.3	137.0	175.4
	20	53.1	144.1	248.4
0.5	5	42.6	111.7	229.9
	10	45.9	128.8	258.0
	15	46.0	138.0	270.7
	20	46.6	142.3	266.7
1	5	42.4	111.6	280.2
	10	45.6	126.6	286.1
	15	45.4	137.4	278.4
	20	50.0	143.0	297.1
2	5	41.5	110.1	283.2
	10	45.8	125.6	291.3
	15	49.0	135.7	297.2
	20	48.6	144.0	312.4

EXPERIMENTAL

Materials

The epoxy resin used in this study was diglycidyl ether of bisphenol A (DGEBA; E51, epoxide equivalent weight = 196 g/equiv, Wuxi Resin Factory, Wuxi, China). The curing agent was Jeffamine T403 (equivalent weight = 81 g/equiv, Huntsman Corp., The Woodlands, TX). The elastomeric toughener used was a liquid ATBN rubber (Hypro 1300 × 16 ATBN, acrylonitrile content = 16 wt %, amine equivalent weight = 874, BF Goodrich Hycar Chemical Group, Akron, OH). The chemical structures of DGEGBA, Jeffamine, and ATBN are shown in Figure 1. Other solvents were all purchased from Nanjing Chemical Reagent Co., Ltd. (Nanjing, China). MWCNT-NH_2s with diameters of 8–15 nm, lengths of about 50 μm, and 0.45 wt % amine groups were supplied by Chengdu Organic Chemistry Co., Ltd. (Chengdu, China).

Sample Preparation

DGEBA and MWCNT-NH_2s were mixed in a 100-mL beaker and sonicated for 2 h at 60°C. Then, 15 phr (parts per hundred resin) ATBN was added, and the mixture was reacted for 20 min with mechanical stirring at 60°C. The mixtures were placed in an oil bath at 75°C. Then, a stoichiometric amount of Jeffamine T403 was added with continuous mechanical stirring until a homogeneous mixture was observed. Several differential scanning calorimetry (DSC) aluminum pans were filled with the reaction mixture. The mixtures (~10 mg) were then cooled and stored in a freezer until they were required for the DSC

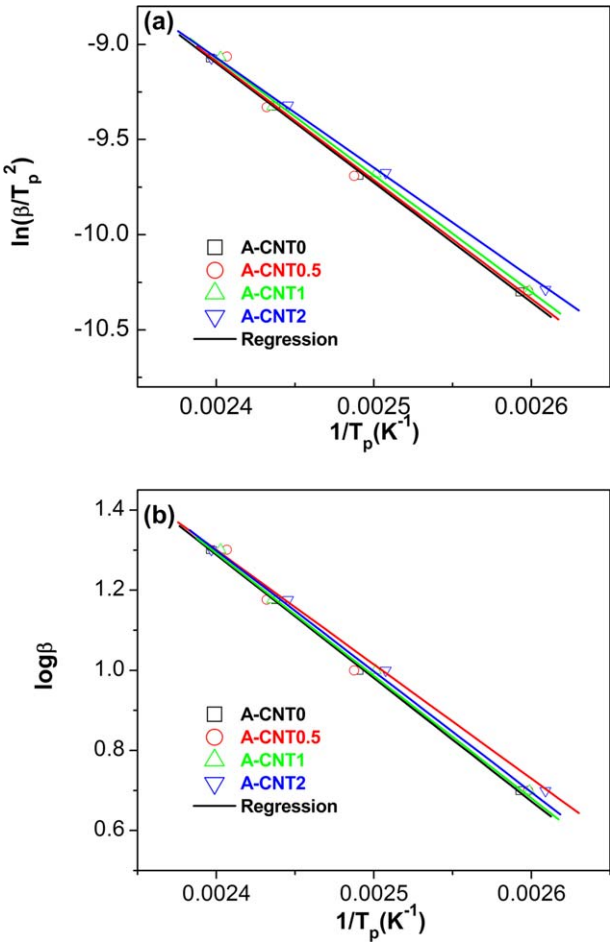

Figure 3. Relationships between (a) $\ln(\beta/T_p^2)$ and $1/T_p$ and (b) $\ln \beta$ and $1/T_p$ for the DGEBA/ATBN/MWCNT-NH_2 nanocomposites. [Color figure can be viewed in the online issue, which is available at wileyonlinelibrary.com.]

measurements. Other mixtures were immediately poured into polytetrafluoroethylene molds and cured for 2 h at 80°C and 3 h at 125°C. DGEBA/ATBN/MWCNT-NH_2 nanocomposites with 0, 0.5, 1, and 2 wt % MWCNT-NH_2s were designated as samples A-CNT0, A-CNT0.5, A-CNT1, and A-CNT2, respectively.

Characterization

DSC. Studies of the dynamic curing kinetics of the epoxy asphalts were performed on a PerkinElmer Pyris 1 DSC instrument (Boston, MA) under an argon flow of 20 mL/min. The samples for kinetic analysis were heated from 50 to 250°C at heating rates (βs) of 5, 10, 15, and 20°C/min, respectively. The T_gs of the cured samples were measured by the Pyris 1 DSC instrument at a β of 20°C/min.

Thermogravimetric Analysis. Thermogravimetric analysis was performed on a Pyris 1 thermogravimetric analyzer (PerkinElmer) with a β of 20°C/min over a temperature range of 25–700°C under a nitrogen flow of 40 mL/min.

Tensile Testing. All of the mechanical tests were performed on an Instron 4466 universal material tester (Norwood, MA) at room temperature at a strain rate of 500 mm/min according to ASTM D 638. The results were averaged over at least six specimens.

Table II. E_α Values for the DGEBA/ATBN/MWCNT-NH_2 Nanocomposites

MWCNT-NH_2 (wt %)	E_α (kJ/mol)	
	Kissinger	FWO
0	52.2	56.0
0.5	51.9	55.6
1	51.1	54.9
2	48.0	51.9

Scanning Electron Microscopy (SEM). SEM images of the fracture surfaces were observed on a Hitachi S-4800 field emission scanning electron microscope. The cured samples were fractured under liquid nitrogen, and then, the fractured surfaces were vacuum-coated with a thin gold layer.

RESULTS AND DISCUSSION

Curing Kinetics

DSC is generally used to monitor the curing behaviors of epoxy resins.[28–30] In this study, dynamic kinetic studies based on the Kissinger and Flynn–Wall–Ozawa (FWO) models[31–33] were used to investigate the DGEBA/ATBN/MWCNT-NH_2 nanocomposites. Both models do not require prior knowledge of the reaction mechanism.

According to the Kissinger model,[31] the activation energy of the reaction (E_α) can be obtained from the following equation:

$$\frac{d[\ln(\beta/T_p^2)]}{d(1/T_p)} = -\frac{E_\alpha}{R} \quad (1)$$

where T_p is the peak exothermal temperature, β is the constant heating rate, and R is the universal gas constant. One can obtain the value of E_α by plotting $\ln T_p^2$ versus $1/T_p$.

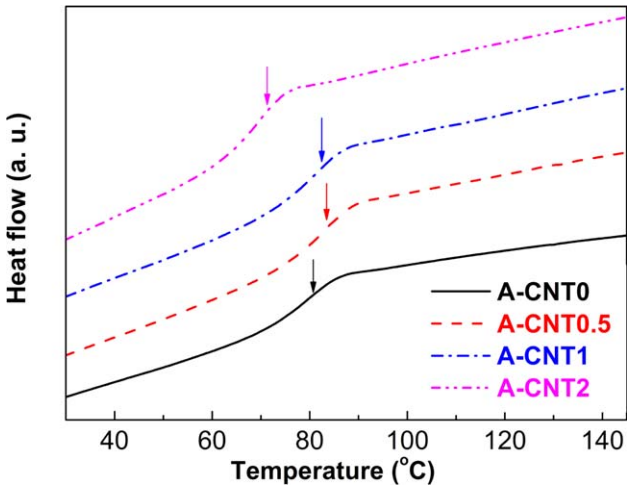

Figure 4. DSC curves for the cured epoxy/ATBN/MWCNT-NH_2 nanocomposites. [Color figure can be viewed in the online issue, which is available at wileyonlinelibrary.com.]

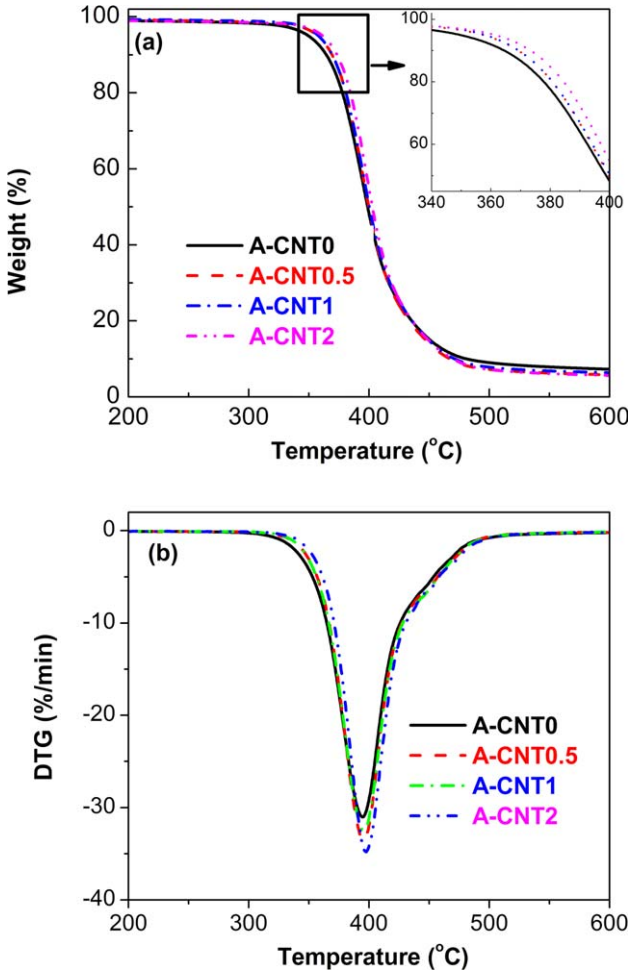

Figure 5. (a) TG and (b) DTG curves for the DGEBA/ATBN/MWCNT-NH_2 nanocomposites. [Color figure can be viewed in the online issue, which is available at wileyonlinelibrary.com.]

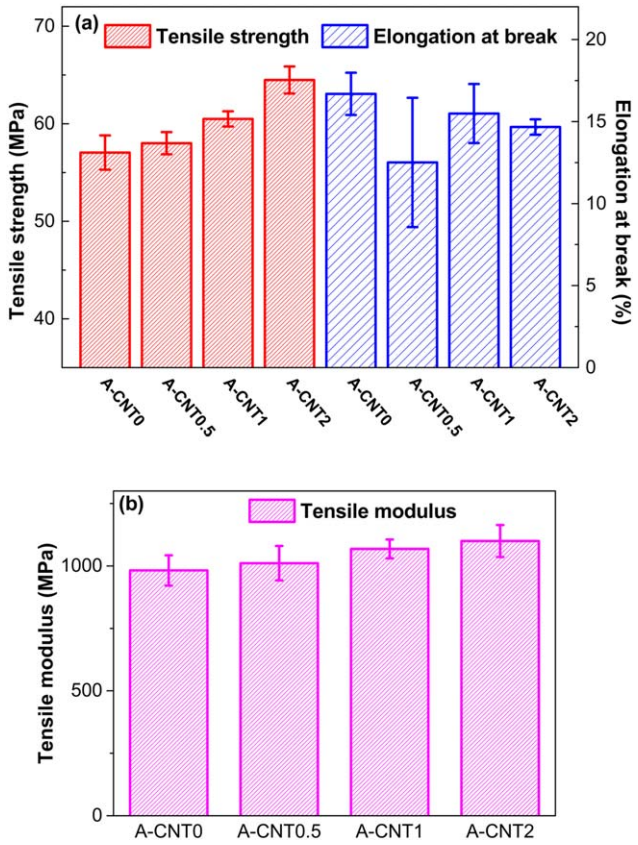

Figure 6. (a) Tensile strength and elongation at break and (b) tensile modulus for the ATBN-toughened epoxy and DGEBA/ATBN/MWCNT-NH_2 nanocomposites. [Color figure can be viewed in the online issue, which is available at wileyonlinelibrary.com.]

The FWO model[32,33] yields a simple relationship between E_α, β, and T_p and gives E_α as follows:

$$\log \beta = A - 0.457 \frac{E_\alpha}{RT_p} \quad (2)$$

Figure 2 shows DSC thermograms from dynamic heating experiments and conversion versus temperature curves for the DGEBA/ATBN/MWCNT-NH_2 nanocomposites conducted at a β of 20°C/min, where the *conversion* is defined as ratio of the heat generated up to time t to the total heat of the reaction. Obviously, the ATBN-toughened epoxy with MWCNT-NH_2s reacted faster than the neat ATBN-toughened epoxy (A-CNT0). Furthermore, the reaction rates of the MWCNT-NH_2 nanocomposites increased with increasing MWCNT-NH_2 content. For the epoxy resin, there are two chemical reactions that form the network: the first between the primary amine and the epoxide group and the second between the secondary amine (formed

Table III. TG and DTG Results for the DGEBA/ATBN/MWCNT-NH_2 Nanocomposites

MWCNT-NH_2 (wt %)	IDT (°C)	T_{max} (°C)
0	350	395
0.5	357	395
1	358	395
2	361	398

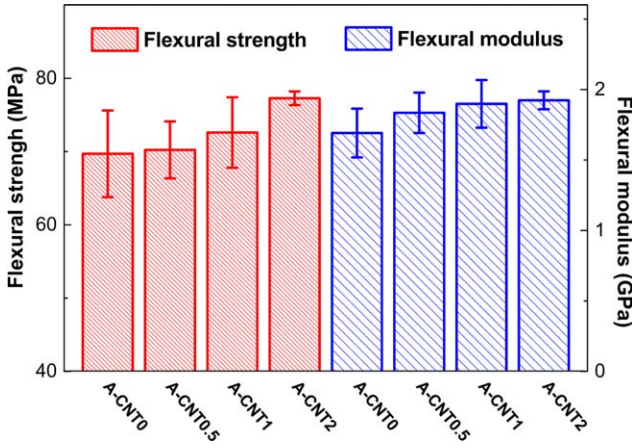

Figure 7. Flexural strength and flexural modulus for the ATBN-toughened epoxy and DGEBA/ATBN/MWCNT-NH_2 nanocomposites. [Color figure can be viewed in the online issue, which is available at wileyonlinelibrary.com.]

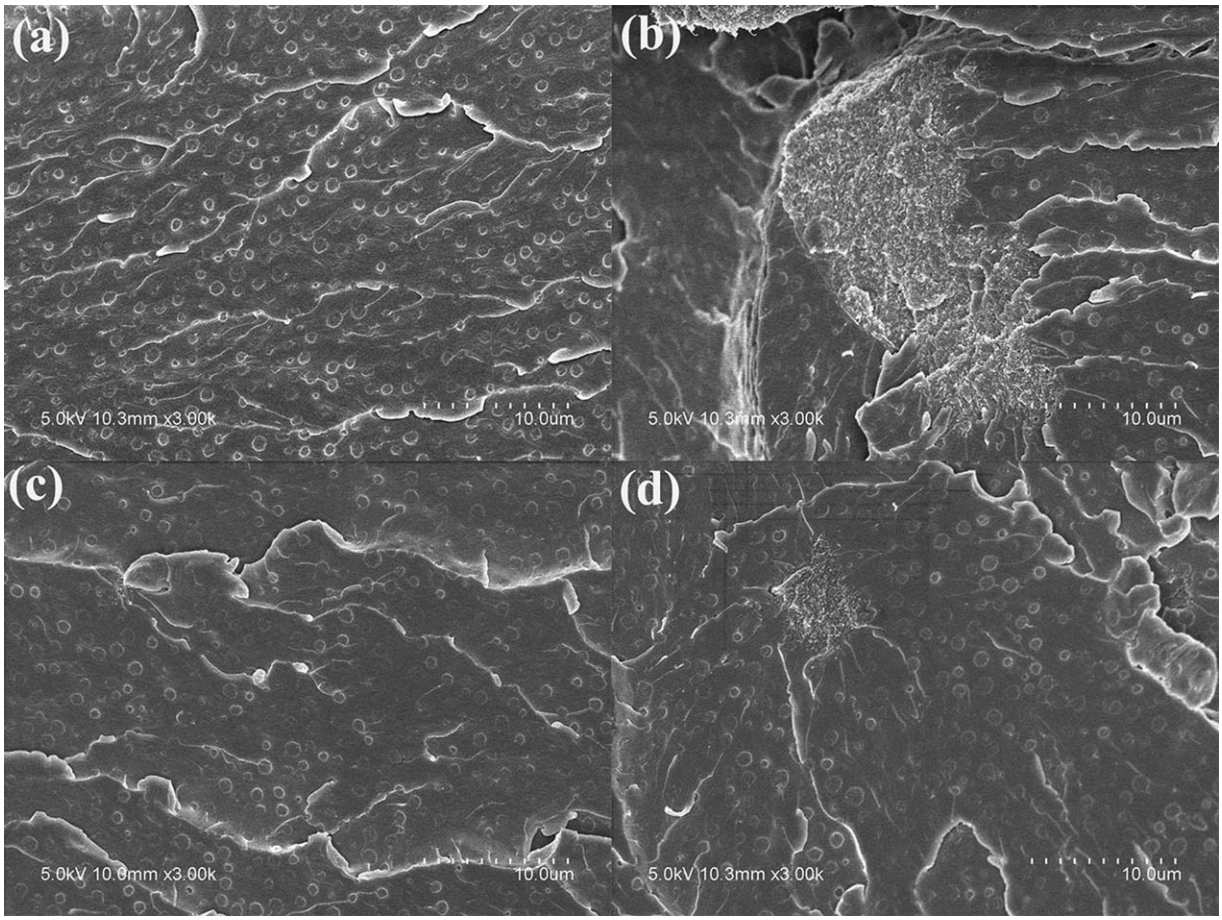

Figure 8. SEM images of the cryofractured surfaces for (a) A-CNT0, (b) A-CNT0.5, (c) A-CNT1, and (d) A-CNT2.

after the removal of one proton by the first reaction) and another epoxide group. It is intuitively expected that the steric hindrance for the second reaction would be much greater than that of the first. Therefore, the stoichiometric amine–epoxy, in which all of secondary amines react with the epoxide, takes longer to complete cure than the amine-excess system.[34] With the addition of amino-functionalized CNTs, the amine was nonstoichiometric. As a result, the curing reaction of the MWNCNT-NH_2 nanocomposites was faster than that of A-CNT0.

The initial reaction temperature (T_i), T_p, and heat of curing (ΔH) of the DGEBA/ATBN/MWCNT-NH_2 nanocomposites at different βs are list in Table I. Both T_i and T_p decreased with increasing MWCNT-NH_2 content; this indicated that the MWCNT-NH_2s acted as a catalyst and facilitated the curing reaction, and the catalytic effect increased with the MWCNT-NH_2 content. Furthermore, ΔH of the DGEBA/ATBN/MWCNT-NH_2 nanocomposites increased with increasing MWCNT-NH_2. This revealed that the amine groups in the MWCNT-NH_2 took part in the curing reaction of the nanocomposites and led to the augmentation of the heat of the curing reaction.

With the Kissinger and FWO methods, the E_α values could be obtained from the slopes of the lines, as presented in Figure 3. Linear relationships were obtained, and this confirmed the validity of the models for the systems under study.

Table II lists the results obtained from the dynamic kinetic analysis. The E_α values obtained from the two models were in good agreement. In addition, the E_α value calculated from the Kissinger model was slightly lower than that of the FWO model; this was consistent with our previous work.[27] It was obvious that the E_α values of the nanocomposites decreased slightly with increasing MWCNT-NH_2 contents. A decrease in E_α suggested that less energy of the reacting components was required and indicated an accelerating effect. This suggested that the addition of MWCNT-NH_2s into the reactive rubber-toughened epoxy facilitated the curing reaction; this was consistent with the results of other workers.[35,36]

T_g

T_g provides an indirect indication of the interfacial adhesion between the nanofillers and the epoxy resin. Reports have revealed that the restricted segmental motion can elevate the T_g of polymer films bonded to solid substrates and filler phases in the composites. The DSC curves of the reactive rubber-toughened epoxy and its MWCNT-NH_2 nanocomposites are shown in Figure 4. The lower loading of the MWCNT-NH_2s had little effect on the T_g of the neat rubber-toughened epoxy. However, the T_g of the 2 wt % MWCNT-NH_2 nanocomposite was about 10°C lower than that of the neat rubber-toughened epoxy. With the increase in the amino-functionalized CNTs, the

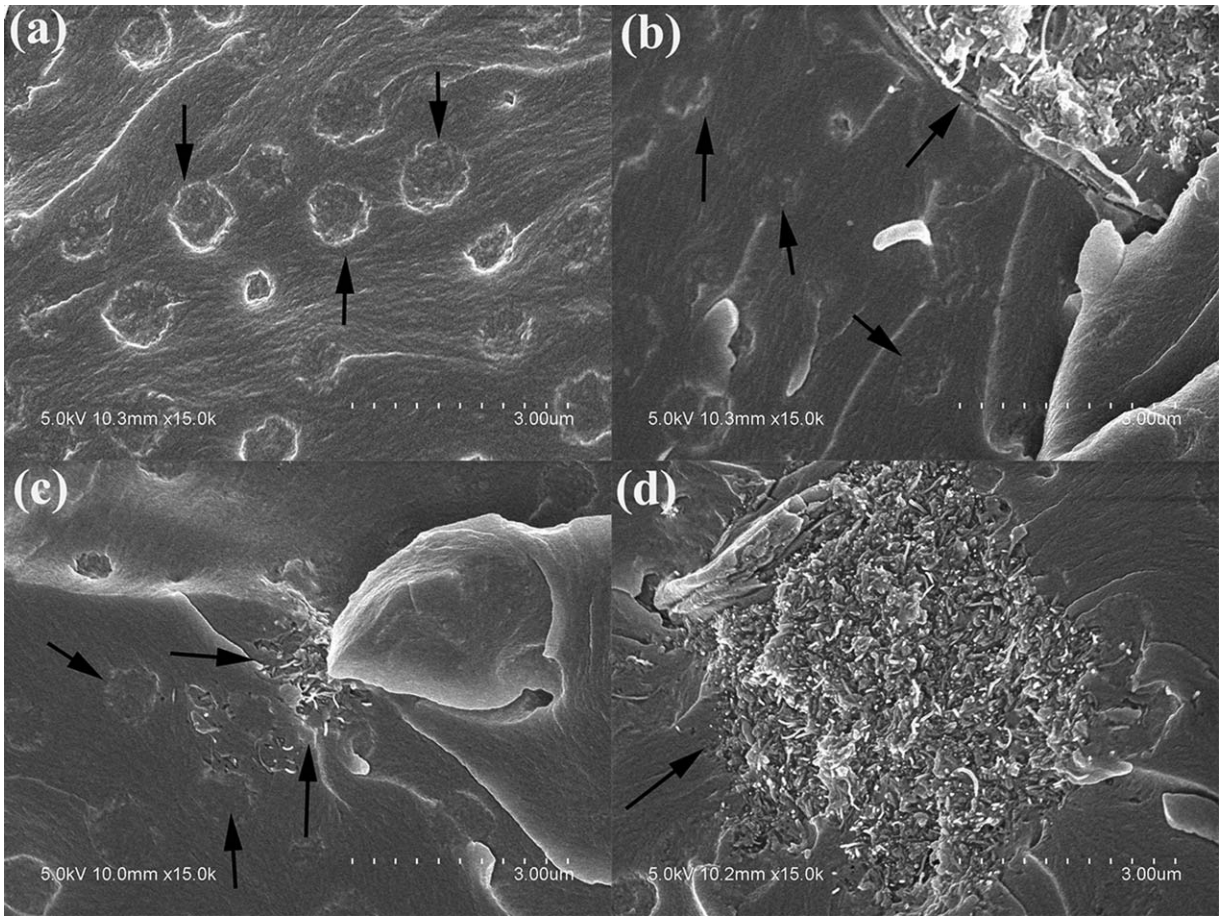

Figure 9. High-magnification SEM images of cryofractured surfaces for (a) A-CNT0, (b) A-CNT0.5, (c) A-CNT1, and (d) A-CNT2.

content of amino groups on the surface of the nanotubes increased. This led to a nonstoichiometric balance between the epoxide group and amino groups. Vallo et al.[37] reported that the T_g of an epoxy–amine system depended on the ratio between the epoxy and the amine. They found that amine-excess systems had lower T_gs than both the stoichiometric system and the epoxy-excess systems. Consequently, the T_g of the nanocomposite decreased with increasing MWCNT-NH_2 contents, and this agreed with the results of a previous report.[38]

Thermal Stability

Thermogravimetry (TG) was used to characterize the amino-functionalized nanotubes on the thermal stability of the DGEBA/ATBN blends. TG and differential thermogravimetry (DTG) curves for the DGEBA/ATBN nanocomposites with different contents of MWNT-NH_2 are shown in Figure 5. The initial decomposition temperature (IDT), which was set as the temperature at the 5% weight loss, and the maximum degradation temperatures (T_{max}) are summarized in Table III. The IDTs of the DGEBA/ATBN/MWCNT-NH_2 nanocomposites increased slightly with increasing MWNT-NH_2 content. As shown in Figure 5(b), every DTG curve showed a single peak at about 395°C that corresponded to the T_{max} for the nanocomposites. The TG results indicate that the addition of MWNT-NH_2 slightly increased the thermal stability of the ATBN-toughened DGEBA systems.

Mechanical Properties

To evaluate the effects of the MWNT-NH_2s on the mechanical properties of the rubber-toughened epoxy, tensile tests and flexural tests were performed, as shown in Figures 6 and 7, respectively. It is well known that the addition of rubber inevitably decreases the tensile strength and modulus and flexural strength and modulus of epoxy resin.[3,8] However, with the addition of the MWNT-NH_2s, the tensile strength and modulus and flexural strength and modulus of the DGEBA/ATBN/MWCNT-NH_2 nanocomposites increased with the nanotube contents, as shown in Figures 6 and 7. Furthermore, the addition of MWNT-NH_2 slightly decreases the elongation at break of the ATBN-toughened epoxy. The mechanical properties of the nanocomposites depended on the dispersion of CNTs in the polymer matrix and the interaction between the CNTs and the polymers.[39,40] In other words, more homogeneous dispersion and a better interface between the nanotubes and the epoxy matrix resulted in better mechanical properties. The mechanical properties of the nanocomposites were not statistically significant; this was attributed to the poor dispersion of the MWCNT-NH_2s in the rubber-toughened epoxy. The dispersion of the amino-functionalized nanotubes are discussed next.

Morphology

SEM microphotographs for the ATBN-toughened epoxy and the various amino-functionalized CNT nanocomposies are displayed in Figures 8 and 9. Phase seperation was obvious in both the rubber-toughened epoxy and its nanotube nanocomposites. However, agglomerates of CNTs for poor dispersion were found in the nanocomposites. Therefore, the interaction between the amino-funcationalized CNTs and rubber-toughened epoxy resin accounted for the improvement in the mechanical properties of the nanocomposites.

CONCLUSIONS

Amino-functionalized CNTs were incorporated into liquid reactive rubber-toughened epoxy resins as a nanofiller. Dynamic kinetic analysis showed that the E_α of the rubber-toughened epoxy nanocomposites decreased slightly with increasing MWNT-NH_2. This indicated that the amino-functionalized nanotubes accelerated the curing reactions of the rubber-toughened epoxy resin. The addition of the MWNT-NH_2s improved the T_g of the rubber-toughened epoxy, whereas the improvement was not linear with the concentration of MWNT-NH_2. The maximum T_g was obtained at the MWNT-NH_2 concentration of 0.5 wt %. The addition of the MWNT-NH_2s enhanced the tensile and flexural properties of the ATBN-toughened epoxy. Furthermore, the tensile and flexural properties of the nanocomposites increased with the nanotube contents. MWNT-NH_2 agglomerations in the viscous ATBN/epoxy system were observed.

ACKNOWLEDGMENTS

The authors are grateful for the financial support of the Opening Funds of the National Engineering Laboratory for Advanced Road Materials, the Program for Changjiang Scholars and Innovative Research Team in University, and the Fundamental Research Funds for the Central Universities (contract grant number 1106020514).

REFERENCES

1. Unnikrishnan, K. P.; Thachil, E. T. *Des. Monomers Polym.* **2006**, *9*, 129.
2. Tripathi, G.; Srivastava, D. *Mater. Sci. Eng. A* **2008**, *496*, 483.
3. Chikhi, N.; Fellahi, S.; Bakar, M. *Eur. Polym. J.* **2002**, *38*, 251.
4. Hodgkin, J. H.; Simon, G. P.; Varley, R. *J. Polym. Adv. Technol.* **1998**, *9*, 3.
5. Chern, Y. C.; Tseng, S. M.; Hsieh, K. H. *J. Appl. Polym. Sci.* **1999**, *74*, 328.
6. Varley, R. *J. Polym. Int.* **2004**, *53*, 78.
7. Thomas, R.; Ding, Y. M.; He, Y. L.; Yang, L.; Moldenaers, P.; Yang, W. M.; Tibor, C.; Thomas, S. *Polymer* **2008**, *49*, 278.
8. Tripathi, G.; Srivastava, D. *Mater. Sci. Eng. A* **2007**, *443*, 262.
9. He, D.; Ding, X. D.; Chang, P. S.; Chen, Q. M. *Int. J. Adhes. Adhes.* **2012**, *38*, 11.
10. Kelnar, I.; Rotrek, J.; Kaprálková, L.; Hromádková, J.; Strachota, A. *J. Appl. Polym. Sci.* **2012**, *125*, 3477.
11. Bokobza, L. *Polymer* **2007**, *48*, 4907.
12. Byrne, M. T.; Gun'ko, Y. K. *Adv. Mater.* **2010**, *22*, 1672.
13. Xie, H. F.; Liu, B. H.; Sun, Q.; Yuan, Z. R.; Shen, J. Y.; Cheng, R. S. *J. Appl. Polym. Sci.* **2005**, *96*, 329.
14. Xie, H. F.; Liu, B. H.; Yang, H.; Wang, Z. L.; Shen, J. Y.; Cheng, R. S. *J. Appl. Polym. Sci.* **2006**, *100*, 295.
15. Chen, S. B.; Wang, Q. H.; Wang, T. M. *Mater. Des.* **2012**, *38*, 47.
16. Wang, C. S.; Chen, X. Y.; Xie, H. F.; Cheng, R. S. *Compos. A* **2011**, *42*, 1620.
17. Xie, H. F.; Liu, B. H.; Yuan, Z. R.; Shen, J. Y.; Cheng, R. S. *J. Polym. Sci. Part B: Polym. Phys.* **2004**, *42*, 3701.
18. Xie, H. F.; Liu, C. G.; Yuan, Z. R.; Yang, H.; Wang, Z. L.; Cheng, R. S. *Acta Polym. Sin.* **2008**, (4), 332.
19. Ma, P. C.; Siddiqui, N. A.; Marom, G.; Kim, J. K. *Compos. A* **2010**, *41*, 1345.
20. Ma, P. C.; Mo, S. Y.; Tang, B. Z.; Kim, J. K. *Carbon* **2010**, *48*, 1824.
21. Gojny, F. H.; Schulte, K. *Compos. Sci. Technol.* **2004**, *64*, 2303.
22. Wang, S. R.; Liang, Z. Y.; Liu, T.; Wang, B.; Zhang, C. *Nanotechnology* **2006**, *17*, 1551.
23. Shen, J. F.; Huang, W. S.; Wu, L. P.; Hu, Y. Z.; Ye, M. X. *Compos. A* **2007**, *38*, 1331.
24. Wang, J. G.; Fang, Z. P.; Gu, A. J.; Xu, L. H.; Liu, F. *J. Appl. Polym. Sci.* **2006**, *100*, 97.
25. Chen, X. H.; Wang, J. F.; Lin, M.; Zhong, W. B.; Feng, T.; Chen, X. H.; Chen, J. H.; Xue, F. *Mater. Sci. Eng. A* **2008**, *492*, 236.
26. Ruiz, M. M. S.; Skordos, A. A.; Partridge, I. K. *J. Mater. Sci.* **2010**, *45*, 2633.
27. Wang, Y. T.; Wang, C. S.; Yin, H. Y.; Wang, L. L.; Xie, H. F.; Cheng, R. S. *Express Polym. Lett.* **2012**, *6*, 719.
28. Qiu, S. L.; Wang, C. S.; Wang, Y. T.; Liu, C. G.; Chen, X. Y.; Xie, H. F.; Huang, Y. A.; Cheng, R. S. *Express Polym. Lett.* **2011**, *5*, 809.
29. Qiu, S. L.; Wang, Y. T.; Wang, C. S.; Yuan, Z. R.; Huang, Y. A.; Xie, H. F.; Cheng, R. S. *Acta Polym. Sin.* **2012**, (1), 25.
30. Yin, H. Y.; Jin, H.; Sun, Y. F.; Yuan, Z. R.; Xie, H. F.; Wang, Z. L.; Cheng, R. S. *J. Therm. Anal. Calorim.* **2014**, *115*, 1073.
31. Kissinger, H. E. *Anal. Chem.* **1957**, *29*, 1702.
32. Flynn, J. H.; Wall, L. A. *J. Polym. Sci. Part B: Polym. Lett.* **1966**, *4*, 323.
33. Ozawa, T. *J. Therm. Anal.* **1970**, *2*, 301.
34. Wasserman, S.; Johari, G. P. *J. Appl. Polym. Sci.* **1994**, *53*, 331.
35. Chen, S.; Hsu, S. H.; Wu, M. C.; Su, W. F. *J. Polym. Sci. Part B: Polym. Phys.* **2011**, *49*, 301.
36. Choi, W. S.; Shanmugharaj, A. M.; Ryu, S. H. *Thermochim. Acta* **2010**, *506*, 77.
37. Vallo, C. I.; Frontini, P. M.; Williams, R. J. J. *J. Polym. Sci. Part B: Polym. Phys.* **1991**, *29*, 1503.
38. Shen, J. F.; Huang, W. S.; Wu, L. P.; Hu, Y. Z.; Ye, M. X. *Compos. Sci. Technol.* **2007**, *67*, 3041.
39. Tasis, D.; Tagmatarchis, N.; Bianco, A.; Prato, M. *Chem. Rev.* **2006**, *106*, 1105.
40. Song, Y. S.; Youn, J. R. *Carbon* **2005**, *43*, 1378.